Identification of A New Kind of Phenazine Compounds Attenuating The Stemness of Breast Cancer Cells Through Triggering Ferroptosis

Yue Yang
China Pharmaceutical University
yuanyuan Lu
China Pharmaceutical University
Chunhua Zhang
China Pharmaceutical University
Qianqian Guo
Henan Cancer Hospital
Ting Wang
China Pharmaceutical University
Zhuolu Xia
China Pharmaceutical University
Jing Liu
China Pharmaceutical University
Xiangyu Cheng
China Pharmaceutical University
Tao Xi
China Pharmaceutical University
Feng Jiang
China Pharmaceutical University
lufeng zheng (zhlf@cpu.edu.cn)
China Pharmaceutical University

Research

Keywords: Breast cancer stem cell, Phenazine compounds, Stemness, Ferroptosis, Iron, Lysosomes

Posted Date: March 1st, 2021

DOI: https://doi.org/10.21203/rs.3.rs-247199/v1

Abstract

Background: Breast cancer stem cells (BCSCs) are positively correlated with metastasis, chemoresistance and recurrence of breast cancer.

Methods: The stemness were analyzed by qPCR and western blot, flow cytometry, cell spheroid formation assay, and tumor xenograft model. The cell viability was performed by MTT. The transcriptome analysis was used to evaluate the influence of these three compounds. The migration was analyzed by wound-healing assay, transwell invasion analysis, and metastasis model. The iron concentration was analyzed by fluorescence microscopy analysis. The lipid peroxidation and ROS level were analyzed by flow cytometry. The results were presented as mean ± SD, the analysis was Student's t-test by using GraphPad Prism 5 software. P-values less than 0.05 were considered to be statistically significant. (*$*p < 0.05, **p < 0.01, ***p < 0.001$*).

Results: Here, we tried to screen out small-molecule compounds targeting BCSCs from the phenazine library established by us before. We focused on the compounds without affecting cell viability and screened out three potential compounds (CPUL119, CPUL129, CPUL149) that can significantly attenuate the stemness of breast cancer cells, as evident by the decrease of stemness marker expression, CD44+/CD24- subpopulation, mammary spheroid-formation ability and tumor-initiating capacity. Additionally, these compounds suppressed the metastatic ability of breast cancer cells *in vitro* and *in vivo*. Combined with the transcriptome-sequencing analysis in breast cancer cells with or without the treatment of these three compounds, respectively, it was found that *ferroptosis* was shown on the top of the most upregulated pathways by CPUL119, CPUL129 and CPUL149. Mechanistically, we found that CPUL119, CPUL129 and CPUL149 could trigger ferroptosis by accumulating and sequestering iron in lysosomes through interacting with iron, and by regulating the expression of proteins (IRP2, TfR1, ferritin) engaged in modulating iron transport and storage. Furthermore, inhibition of ferroptosis rescued the suppression of these three compounds on the stemness of breast cancer cells.

Conclusions: This study suggests that CPUL119, CPUL129 and CPUL149 can specifically inhibit the stemness of breast cancer cells through ferroptosis and may be the potential compounds for breast cancer treatment.

Background

Cancer stem cells (CSCs) have been considered as a root of cancer progression[1-3]. Breast cancer displays characteristics of recurrence, metastasis and chemoresistance because of its heterogeneity, which could be contributed by BCSCs[4]. Targeting BCSCs has been considered as a potential way for breast cancer treatment. However, there are still no drugs targeting BCSCs approved for clinical using in breast cancer treatment.

Many signaling pathways such as Wnt, Hedgehog and Hippo, have been confirmed to be critically involved in BCSC progression[5]. Small molecular compounds and biologics have been better developed

in the process of targeting CSCs, such as Glasdegib targeting leukemia stem cells (LSCs)[6] and ELZONRIS targeting CD123 that is highly expressed in LSCs have already been approved by the USA Food and Drug Administration (FDA)[7]. However, there are still no drugs targeting BCSCs approved for clinical application in breast cancer treatment. Thus, finding new compounds or through drug repositioning to find compounds targeting BCSCs is becoming more and more important.

Recently, the iron metabolism has been found to be dysregulated in BCSCs[8]. The iron level is increased in the BCSCs, which causes the BCSCs to be more sensitive to iron chelation[9]. The existence of iron could directly change the cell differentiation, and the loss of transferring iron to lysosome could increase the stemness of cancer cells[10]. Iron also could produce $OH^{\cdot}$ through inducing Fenton reaction which was the strongest oxygen-free radical in the reactive oxygen species (ROS), and the $OH^{\cdot}$ can attack lipid to increase lipid peroxidation, which is one critical contributor of ferroptosis[5]. Additionally, the iron homostasis is modulated by different iron regulatatory proteins, such as iron-responsive element binding protein 2 (IRP2), transferrin receptor 1 (TfR1) and ferritin. IRP2 could bind to the iron regulator element (IRE) of mRNA 3'UTRs (untranslation region) or 5'UTRs of the different iron regulatory genes to stabilize or degrade the mRNAs[11]. TfR1 and transferrin degradation in lysosomes have been shown to be increased in BCSCs, while ferroportin (FPN) is decreased[12]. The decrease of transferrin leads to a suppression of ROS and ferroptosis[13]. Ferritin is the container to store iron and superoxide radicals could trigger the Fe^{2+} release from the ferritin[14]. The use of lysosome disruptor, siramesine, could increase the iron in breast cancer cells resulting in the increase of ROS and ferroptosis[13]. Besides, the induction of ferroptosis is accompanied by the degradation of ferritin[15].

It was found that the decrease of iron concentration in lysosomes could maintain the stemness of cancer cells[16]. The decrease of iron output-related gene and the increase of iron input-related gene represent a better prognosis in breast cancer[17]. Recently, iron nanoparticles that could target CSCs through ferroptosis and apoptosis were approved by the FDA, which bring up a new strategy to treat cancer by applying iron[18]. These results suggest that the iron increase in BCSCs promotes the activity of iron-dependent proteins and avoids the damage caused by iron overload through reducing the iron reserve in the lysosomes, thus reaching an "adjusted iron homeostasis" in line with the CSC metabolism level. Consistently, it has been shown that salinomycin and its drivatives could target BCSCs through sequestering iron in lysosomes[19-21]. Notably, targeting iron in lysosomes has been confirmed to killing CSCs in other tumors, such as nasopharyngeal carcinoma[22] and colorectal cancer[23]. These results amplify that sequestering iron in lysosomes is a promosing method in targeting BCSCs.

In the present study, we reported three phenazine compounds (CPUL119, CPUL129, CPUL149) that can significantly attenuate the stemness of breast cancer cells through sequestering iron in lysosomes by interacting with and sequestering iron in lysosomes and thus triggering ferroptosis. This study indicates that CPUL119, CPUL129 and CPUL149 maybe the potential drugs for breast cancer treatment through attenuating the stemness of breast cancer cells.

Methods

Cell culture

Human breast cancer cell lines including MCF-7 cells, MDA-MB-231 cells and Adriamycin resistant MCF-7-Adr cells were stored in our laboratory. The MCF-7 and MDA-MB-231 cells were cultured in DMEM medium (KeyGEN, Cat# KGM12800-500) with 10% fetal bovine serum (FBS, BI, Cat# 04-001-1ACS). MCF-7-Adr cells were cultured in 1640 medium (KeyGEN, Cat# KGM31800-500) with 10% fetal bovine serum. All the cell culture contamination was at 37 °C under a humidified atmosphere with 5% CO2.

Reagents

Z-VAD-FMK (APExBIO, Cat# A1902), Necrostatin-1 (APExBIO, Cat# A4213), Ferrostatin-1 (APExBIO, Cat# A4371), NAC (Beyotime, Cat# S0077), CA-074 methyl ester (MCE, Cat# HY-100350), Ammonium ferric citrate (Sigma, Cat# F5879), Deferoxamine mesylate salt (YuanyeBio, Cat# S61301)

Quantitative Real-time PCR (qPCR)

The process of this experiment was referred to our previous study[24].

Western blot

The cells were collected by 1×PBS (phosphate buffer saline) (diluted with double distilled water, Servicebio, Cat# G4207-500ML) and were lysed with RIPA Lysis Buffer (Beyotime, Cat# P0013B) with PMSF (1:100, Beyotime, Cat# ST506) on the ice. After SDS-PAGE (sodium dodecyl sulfate – polyacrylamide gel electrophoresis) analysis, the proteins were transferred on the PVDF (polyvinylidene fluoride) membranes (Millipore, Cat# IPVH00010), which were then incubated with the primary antibodies at 4℃ overnight. The membranes were incubated with the secondary antibodies (Goat Anti-Rabbit IgG (H+L), HRP conjugate; Goat Anti-Mouse, IgG (H+L), HRP conjugate, proteintech, Cat# SA00001-2, Cat# SA00001-1) and protein signals were detected with High-sig ECL Western Blotting Substrate (Tanon, Cat# 180-5001) on Tanon5200. The antibody used in this study including ALDH1A1 (Proteintech,15910-1-AP), OCT3/4 (Wanleibio, Cat# WL01728), GAPDH (Proteintech, Cat# 60004-1-l g), E-cadherin (Proteintech, Cat# 20874-1-AP), N-cadherin (Proteintech, Cat# 22018-1-AP), MMP9 (Affinity, Cat# AF5228), IRP2(Proteintech, Cat# 23829-1-AP), TfR1 (Santa, Cat# SC-32272), ferritin (Abcam, Cat# ab75973).

Flow Cytometry Analysis

MCF-7 and MDA-MB-231 cells were seeded into 6-well plates and treated with different compounds or inhibitors, after 48 h, the cells were stained with Hu CD44 APC (BD Pharmingen, Cat# 559942) and Hu CD24 BV421(BD Pharmingen, Cat# 562789) on the ice in 30 min and then the subpopulation of CD44+/CD24- ratio was analyzed on a MACSQuant flow cytometer (Miltenyi Biotec).

Cell spheroid formation assay

MCF-7 and MDA-MB-231 cells were seeded into low-adherent 24-well plates at a density of 3000 - 5000 cells/well and cultured with the MammoCult™ Human Medium Kit (stemcell, Cat# 05620) supplemented with compounds for 8 days. Then spheroid number was calculated and size was measured under a microscope (Leica).

MTT

Cell viability was measured by MTT (Solarbio, Cat# M8180-250 mg). MCF-7, MDA-MB-231 and MCF-7-Adr cells were seeded into 96-well plates at a density of 3000 - 5000 cells/well. After 24 h, different concentrations of CPUL119, CPUL129 and CPUL 149 were added. 48 h later, 20 μl 5 mg/ml MTT was added into the medium for a 4 h culturing. Then the medium was removed and added 150 μl DMSO into each well. After shocking for 10 min, the absorbance at 490 nm was analyzed on a Biorad iMark.

Detection of Lipid peroxidation

MCF-7 and MDA-MB-231 cells were seeded into 6-well plates. After 24 h, cells were treated with compounds (4.5 μM CPUL119, 1.8 μM CPUL129 and 0.9 μM CPUL149), NAC (5 mM), and DFO (2 μM). 48 h later, the cells were stained with 10 μM Lipid peroxidation sensor (ThermoFisher, Cat# B3932) for 30 min at 37℃. Then lipid peroxidation level was analyzed with a flow cytometer.

Detection of ROS level

MCF-7 and MDA-MB-231 cells were seeded into 6-well plates. After 24 h, cells were treated with compounds (4.5 μM CPUL119, 1.8 μM CPUL129 and 0.9 μM CPUL149). 48 h later, the production of ROS was analyzed by reactive oxygen species assay kit (Beyotime, Cat# S0033S) through a flow cytometer.

GSH determination

The analysis of GSH was performed by Micro Reduced Glutathione (GSH) Assay Kit (Solarbio, Cat# BC1175) following the manufacturer's recommendation.

Analysis of iron content

The content of iron in the cell was measured by Iron Colorimetric Assay Kit (Applygen, Cat# E1042-100) according to the standard protocol. Briefly, MCF-7 and MDA-MB-231 cells were seeded into 24-well plates. After 24 h, the cells were treated with compounds (4.5 μM CPUL119, 1.8 μM CPUL129 and 0.9 μM CPUL149). 48 h later, the iron concentration was analyzed by Iron Colorimetric Assay Kit.

Wound-Healing assay

MCF-7 and MDA-MB-231 cells were seeded into 6-well plates and cultured in the complete medium until growing up to 90%. Then, a wound was produced on the cell surface, and washed it with PBS twice to remove the cell fragments. Cells were cultured in the medium with low serum concentration(≤2%) contained compounds or solvent. After 24 h and 48 h, the wounds were observed and taken with a

microscope. Migration rate = $(D_t-D_0) / D_0$, the D_t represents the distance between the wound at different times.

Invasion assay

Cell invasion ability was assayed by transwell invasion analysis. Finally, the Millicell Hanging cell culture inserts (Merck, Cat# MCEP24H48) coated with Matrigel matrix (Corning, Cat# 356234) were prepared in the 24-well plates. The 2×10^5 MCF-7 or MDA-MB-231 cells with 200 μl serum-free medium with different compounds or solvent were added into the upper chamber, and the lower chamber was filled with medium containing 20% serum. After 48 h, the cells were fixed with 70% ethanol for 20 min at room temperature. Then, the invaded cells were stained with crystal violet staining solution (Beyotime, Cat# C0121-100 ml), and observed under a microscope. After then, the chambers were washed with 33% glacial acetic and the absorbance at 570 nm was analyzed on a Biorad iMark, which represents the invaded cell number.

Fluorescence Microscopy Analysis

MCF-7 cells were seeded into glass-bottom culture dishes (NEST, Cat# 801001) to carry on this experiment. After 24 h, these cells were treated with different compounds (4.5 μM CPUL119, 1.8 μM CPUL129 and 0.9 μM CPUL149). 48 h later, the cells were stained with different probes as the following methods. 50 nM LysoTracker Deep Red (ThermoFisher, Cat# L12492) was incubated with cells for 90 min at 37℃. 50 nM MitoTracker Deep Red (ThermoFisher, Cat# M22426) was incubated with cells for 30 min at 37℃. 1 μM FerroOrange (DOJINDO, Cat# F374) was incubated with cells for 30 min at 37℃. 2 μg/ml Hoechst 3342 was incubated with cells for 30 min at 37℃. After stained with different probes, we used a LSM800 to analyze.

RNA sequencing and data analysis

RNA sequencing and data analysis were performed by Novogen (Beijing, China).

Tumorigenesis *in vivo*

The BALB/c-nude mice (Gempharmatech, Cat# D000521) were female, 3-4 weeks, and were cultured in standard pathogen-free conditions. Each group had six mice. All the experiments were obtained the approval of the Ethics Committee for Animal Experimentation of China Pharmaceutical University. In the tumor-limiting dilution assay, 1×10^6, 1×10^5 and 1×10^4 MCF-7 and MDA-MB-231 cells pre-treated with compounds (4.5 μM CPUL119, 1.8 μM CPUL129 and 0.9 μM CPUL149) for 48 h were implanted in the inguinal mammary gland of mice orthotopically. After 10 days, the mice were sacrificed, and the amounts of tumors in each group were counted. And the stem cell frequencies were analyzed by ELDA (http://bioinf.wehi.edu.au/software/elda/).

Metastasis *in vivo*

The BALB/c-nude mice (Gempharmatech, Cat# D000521) were female, 3-4 weeks, and were cultured in standard pathogen-free conditions. Each group had five mice. All the experiments were obtained the approval of the Ethics Committee for Animal Experimentation of China Pharmaceutical University. In the metastasis, each mouse was injected with 2×10^6 MDA-MB-231 cells by intravenous. One week later, these mice were injected with different compounds (10 mg/kg 119, 10 mg/kg 129, 5 mg/kg 129) or solvent (23.7% ethanol, 17%PEG400, 59.3% saline) intravenous every two days. After one month later, the mice were sacrificed. And the lungs were made H&E by Servicebio.

Statistical analysis

The results were presented as mean ± SD, the analysis was Student's t-test by using GraphPad Prism 5 software. P-values less than 0.05 were considered to be statistically significant. (*$p < 0.05$, **$p < 0.01$, ***$p < 0.001$*).

Results

Identification of CPUL119, CPUL129 and CPUL149 as novel small-molecules suppressing breast cancer cell stemness

We tried to screen out potential compounds that can specifically attenuate the stemness of breast cancer cells without affecting cell viability from the phenazine-compound library we established before[25]. It was found that nine compounds (W23, W24, W49, W53, CPUL116, CPUL124, CPUL119, CPUL129, CPUL149) had little effect on breast cancer cell viability (**Table1**), which were chosen for the further studies. As shown in **Figure 1A-1I**, the compounds (W23, W53, CPUL116, CPUL119, CPUL129, CPUL149) exhibited a certain suppressing effect on the mRNA expression of stemness markers (SOX2, Oct4, Nanog, ALDH1A1) in a concentration-dependent manner. However, only compounds (CPUL119, CPUL129, CPUL149) decreased the protein expression of stemness markers in a concentration-dependent manner without affecting cell viability (**Figure 1J** and **1K**). The structures of these three compounds were shown in **Figure 1L**. Furthermore, CPUL119, CPUL129 and CPUL149 had no effect on breast cancer cell viability (**Figure 1M** and **1N**).

Additionally, we conducted the transcriptome sequencing in breast cancer cells with or without CPUL119, CPUL129, CPUL149 treatment, respectively. As shown in **Figure 2A-2C**, the transcription of stemness-related genes (such as UCA1[26], MALAT1 [27]) was suppressed in cells treated with these three compounds, respectively. Moreover, Gene Set Enrichment Analysis (GSEA) demonstrated that multiple signaling pathways related to stem cell differentiation were enriched in cells treated with these three compounds, respectively (**Supplement Figure S1** and **S2**). To further confirm the effects of CPUL119, CPUL129 and CPUL149 on the stemness of breast cancer cells, we conducted western blot experiments in another two breast cancer cell lines (MDA-MB-231 and MCF-7-Adr) and obtained the consistent results (**Figure 3A** and **3B**). In addition, the CD44+/CD24- cell-subpopulation with stemness was decreased by these three compounds (**Figure 3C** and **3D**). Furthermore, CPUL119, CPUL129 and CPUL149 significantly

suppressed the mammary spheroid-formation ability which is positively correlated with cancer cell stemness, as characterized by the decrease of spheroid size and number (**Figure 3E** and **3F**). These results suggest that the compounds CPUL119, CPUL129 and CPUL149 can inhibit the stemness of breast cancer cells *in vitro*.

Table 1. The information of compounds

Number	Molecular weight	IC50 in MCF-7
W23	605.2288	>50
W24	646.1632	50
W49	645.1195	33.24±2.29
W53	605.2288	>50
116	446.89	11.02±0.83
119	444.28	21.23±5.78
124	455.47	nd.
129	460.46	nd.
149	481.33	nd.

CPUL119, CPUL129 and CPUL149 inhibit the migration, invasion and drug resistance of breast cancer cells

As CSCs have regarded as one of a root of tumor metastasis and drug resistance, we continue to investigate the effects of CPUL119, CPUL129 and CPUL149 on the migration, invasion, epithelial-mesenchymal transition (EMT) process and drug resistance of breast cancer cells. Firstly, it was found that these three compounds could inhibit the expression of metastasis-related genes and drug resistance based on the transcriptome-sequencing analysis (**Figure2A** and **Supplementary Figure S3**). We then performed the wound-healing assay to determine whether these three compounds could influence the migration ability of breast cancer cells. As shown in the **Figure 4A** and **4B**, cell migration ability was restrained after being treated with these three compounds for 24 h and 48 h. The invasion ability of breast cancer cells was also inhibited by these three compounds for 48 h (**Figure 4C** and **4D**). Additionally, it was found that the protein expression of epithelial marker (E-cadherin) was increased, while N-cadherin and MMP-9 expression was decreased by these three compounds (**Figure 5A**). Moreover, the effects of these three compounds on drug resistance were further explored. Since paclitaxel (Taxol) and Adriamycin (Adr) are the first-line drugs for breast cancer, we chose them as the research subjects. As shown in **Figure 5B** and **5C**, compared to the cells that only treated with Taxol or Adr alone, a distinct decrease of IC50 values of Taxol and Adr was observed in cells treated with Taxol or Adr as well as

CPUL119, CPUL129 or CPUL149, respectively. Thus, our results demonstrate that CPUL119, CPUL129 and CPUL149 can attenuate the metastasis and drug resistance of breast cancer cells *in vitro*.

CPUL119, CPUL129 and CPUL149 inhibit the stemness and metastasis of breast cancer cells *in vivo*

We then evaluated the tumor-initiating ability of MCF-7 and MDA-MB-231 cells pre-treated with or without CPUL119, CPUL129 or CPUL149, respectively. As shown in **Figure 6A-6F**, the tumor-initiating ability was decreased by the pre-treatment of CPUL119, CPUL129 or CPUL149, which was characterized by the decreased tumor-formation rate and confidence intervals for 1/ (stem cell frequency). Notably, CPUL129 just impaired the tumor-initiating ability of MCF-7 cells in the high concentration of injected cell number, this result suggested CPUL129 may not inhibit the stemness of breast cancer cells *in vivo*, at least in the lower cell concentrations. Additionally, we constructed a lung metastatic model through injecting MDA-MB-231 cells by tail intravenous in nude mice. After one week, these nude mice were treated with CPUL119, CPUL129 and CPUL149 by tail intravenous every three days, respectively. One month later, these mice were sacrificed (**Figure 7A**). As shown in **Figure 7B** and **7C**, through H&E staining analysis, mice treated with these three compounds had smaller and fewer lung metastatic nodules compared with control mice which were treated with the solvent. Importantly, the groups treated with these three compounds exhibited a healthier phenotype by detecting mice weight (**Figure 7D**). Consequently, these results demonstrate that CPUL119, CPUL129 and CPUL149 can inhibit the stemness and metastasis of breast cancer cells *in vivo*.

CPUL119, CPUL129 and CPUL149 regulates the iron hemostasis and ferroptosis in breast cancer cells

To explore the underlying mechanisms underlying the effects of CPUL119, CPUL129 and CPUL149 on the stemness of breast cancer cells, we re-analyzed the transcriptome-sequencing datasets and found that the *ferroptosis (HSA04216)* was significantly enriched in cells treated with these three compounds, respectively (**Figure 8A-8C**). Consistently, GO analysis revealed that some biological process related lysosome function and iron transport were enriched, such as *lysosomal lumen, iron-sulfur cluster assembly, protein maturation by iron-sulfur* (**Supplementary Figure S4-6**). KEGG pathway analysis showed that *glutathione (GSH) metabolism*, which is also involved in ferroptosis, was enriched too (**Supplementary Figure S4-6**). Firstly, we detected the effects of these three compounds on GSH levels; however, it was found that GSH level was not changed by the treatment of these three compounds, respectively (**Figure 9A**). Then, we evaluated iron concentration in breast cancer cells with or without treatment of CPUL119, CPUL129 or CPUL149, respectively and found that the iron concentration was significantly increased by these three compounds (**Figure 9B**). Furthermore, we examined the effect of these compounds on iron homestasis. Treatment of cells with CPUL119, CPUL129 or CPUL149 induced a response trait of cytoplasmic deletion of iron, which was characterized by the increase of TfR1 and IRP2 along with decreased ferritin expression (**Figure 9C-9F**). Besides, an increase of labile iron was observed

in cells treated with these three compounds, respectively (**Figure 10A**). Besides, the compounds may have a combination with iron in MCF-7 cells according to the Colocalization coefficient Rr (**Figure 10B**). There are two factors regulating lipid peroxides during ferroptosis, including GSH and iron concentration[5]. As our previous results showed that CPUL119, CPUL129 or CPUL149 had no effect on GSH level, we wondered whether the increased iron concentration could increase the production of lipid peroxides. Indeed, the ROS was increased in cells treated with these three compounds, respectively (**Figure 10C** and **10D**). Besides, the GO analysis is enriched genes-associated with oxidation-reduction process such as *Oxidoreductase activity* (**Supplementary Figure S5**). Furthermore, the lipid peroxidation was increased by the treatment of these three compounds (**Supplementary Figure S7 A-D**).

CPUL119, CPUL129 and CPUL149 interact and sequester iron in lysosomes in breast cancer cells

We wondered whether CPUL119, CPUL129 and CPUL149 are located in lysosomes. As shown in **Figure 11A** and **11B**, CPUL119, CPUL129 and CPUL149 were located in lysosomes, while a few of them were also located in mitochondria which plays a critical role in oxidative metabolism[28], demonstrating that these three compounds mostly accumulate in lysosomal compartment. Additionally, it was found that CPUL119, CPUL129 and CPUL149 interacted with iron and led to the iron aggregation in lysosome, while iron was diffused in the cytosol of untreated-cells (**Figure 11C** and **11D**). These data indicated that CPUL119, CPUL129 and CPUL149 can interact and induce iron aggregation in lysosome.

CPUL119, CPUL129 and CPUL149 attenuate the stemness of breast cancer cells partially through triggering ferroptosis

Finally, we investigated whether CPUL119, CPUL129 and CPUL149 attenuate the stemness of breast cancer cell through triggering ferroptosis. To determine whether other cell death pathways, including necrosis and apoptosis, which are commonly engaged in lysosomal cell death are involved in these three compound-mediated inhibitions on breast cancer cell stemness, apoptosis inhibitor Z-VAD-FMK, necrosis inhibitor Nec-1, ferroptosis inhibitor Fer-1, or ROS scavenger NAC were added in cells with CPUL119, CPUL129 or CPUL149 treatment respectively. As shown in **Figure 12A**, ferroptosis inhibitor or ROS scavenger NAC, but not Z-VAD-FMK or Nec-1, rescued the suppression of CPUL119, CPUL129 or CPUL149 on stemness marker expression. Additionally, the decreased subpopulation of CD44+/CD24- ratio led by CPUL119, CPUL129 or CPUL149 was partially abrogated by Fer-1 or NAC, respectively (**Figure 12B-12C)**. Furthermore, a consistent result was obtained when the spheroid formation ability was evaluated (**Figure 12D and 12E**). Besides, we explored whether the effects of CPUL119, CPUL129 or CPUL149 on the stemness of breast cancer cells was indeed dependent on lysosome function or iron. CA-074 (an inhibitor of the lysosomal protease cathepsin B) or iron chelating agent deferoxamine (DFO) was added in cells treated with these three compounds, respectively. As shown in **Supplementary Figure S7A-D**, the increased lipid peroxides led by these three compounds was attenuated by CA-074, and enhanced by DFO. Consistently, CA-074 rescued the effects of CPUL119, CPUL129 and CPUL149 on the expression of

ferritin and stemness markers (**Figure 13A** and **13B**). These above results link the lysosomal degradation of ferritin to the production of ROS in this organelle through the release of additional soluble redox-active iron, thus attenuating the stemness of breast cancer cell stemness. Ferric ammonium citrate (FAC) was added into breast cancer cells to increase the iron concentration and the results indicated that FAC indeed promoted the expression of stemness markers and ferritin and even reversed the effects of CPUL119, CPUL129 and CPUL149 on the expression of ferritin and stemness markers (**Figure 13C** and **13D**). Overall, our results demonstrate that CPUL119, CPUL129 and CPUL149 suppress the stemness of breast cancer cells through sequestering iron in lysosomes and triggered ferroptosis.

Discussion

BCSCs have been considered to be the root of breast cancer progression, thus, targeting BCSCs maybe a promising way to treat breast cancer thoroughly [4, 29-31]. In the present work, we aim to screen out small-molecule compounds targeting BCSCs from the phenazine library established by us before. We finally screened out CPUL119, CPUL129 and CPUL149 as promosing compounds which can specifically attenuating the stemness of breast cancer cells without affecting cell viability, as evident by the ability to reduce the stemness, invasion and chemoresistance *in vitro* and *in vivo*, and CPUL149 showed a better activity among the three compounds.

Targeting the abnormal signaling pathways, such as Wnt, Notch, Hedgehog and autophagy, has been shown to potentially killing CSC as we reviwed in a recent study[5], however, most of small-molecule compounds are just in the preclinic stage. Targeting iron metabolism using the iron nanoparticles can be used to treat cancer through ferroptosis, which has been approved by FDA[32]. Besides, inducing ferroptosis through sequenstering iron in lysosome has been confirmed to specifically killing CSCs including BCSCs[10, 20, 22, 23]. In this work, we found CPUL119, CPUL129 and CPUL149 could increase the content of iron in breast cancer cells accompanying with the change of iron-regulatory protein such as IRP2, TfR1 and ferritin. Specifically, these three compounds can interact, induce iron aggregation in lysosome and thus trigger ferroptosis. We noted that although iron in lysosomes could be further increased after the treatment of these compounds, iron also locates in lysosomes in the normal situation (**Figure 11C** and **11D**), this indicates an iron-rich environment in lysosomes[33]. Additionally, the decreased stemness resulted by these three compounds was attenuated or even reversed by ferroptosis inhibitor (fer-1), NAC and ferritin degradation inhibitor (CA-074), and the stemness was increased if we used the FAC to increase the iron. Notably, a small number of CPUL119, CPUL129 and CPUl149 were located in mitochondria which plays a critical role in oxidative metabolism, and apoptosis or necrosis inhibitor could also resuced the effects of these three compounds on the stemness of breast cancer cells although without significance. The GO analysis enriched necrosis correlated biological processes such as *tumor necrosis factor receptor and tumor necrosis factor receptor binding* (**Supplementary Figure S2A)**. These results suggest that CPUL119, CPUL129 or CPUL149 might suppress the stemness of breast cancer cells

through other signaling pathways, or these three compounds suppress the stemness of breast cancer cells through different signaling pathways as shown in the GO- or KEGG-enrichment analysis. Furthermore, since cancer cells can be transformed into CSCs under certain conditions[34, 35], the effects of apoptosis or necrosis inhibitor on the stemness of breast cancer cells might be led by the effects on cancer cells. Moreover, we determined the location of these compounds only using lysosome probe and mitochondrion probe, and other organelle probes, such as endoplasmic reticulum or Golgi apparatus, was not used. Therefore, it is still unclear whether CPUL119, CPUL129 and CPUL149 locate in other organelles. Finally, supplementing with FAC enhanced the stemness of breast cancer cells, this is consistent with the previous study indicating that glioblastoma stem-like cells prefer to iron trafficking[36].

Although the compounds target BCSCs through ferroptosis have been shown to have better research trend and anti-BCSCs ability, the risks should be considered. At first, the iron metabolism is very vital in hematologic, cardiomyopathy and liver[37-39], thus the iron overload maybe cause the unpredictable effects to this system; however, these three compounds may have no effect on hematopoietic system as a healthier phenotype was observed in mice treated with these three compounds by detecting mice weight (**Figure 7D**). Besides, once the ferroptosis happens, abundant oxidative substance can be produced, such as OH·, these oxidative substances maybe attack the normal tissue. Therefore, these reasons may be challenging to make these compounds in the clinic, and more experiments are still needed. Notably, this study demonstrates that these three compounds may act as iron chelators, this speculation should be confirmed by other experiments, such as Nuclear Magnetic Resonance (NMR), and the detailed binding sites should be further explored.

Although these compounds showed better activity target BCSCs in the laboratory, we didn't take any pharmacodynamics, pharmacokinetics and toxicological evaluation. So, these may cause these compounds to face the challenge to be a drug. But these three compounds maybe become lead compounds to further enrich the library of molecules targeting BCSCs because of their better anti-stemness activity.

Conclusions

This study suggests that CPUL119, CPUL129 and CPUL149 can specifically inhibit the stemness of breast cancer cells through ferroptosis and may be the potential compounds for breast cancer treatment.

Abbreviations

BCSCs: Breast cancer stem cells

CSCs: Cancer stem cells

LSCs: leukemia stem cells

FDA: Food and Drug Administration

ROS: reactive oxygen species

IRP2: iron-responsive element binding protein 2

TfR1: transferrin receptor 1

IRE: iron regulator element

FPN: ferroportin

GSEA: Gene Set Enrichment Analysis

EMT: epithelial-mesenchymal transition

Taxol: paclitaxel

Adr: Adriamycin

GSH: glutathione

FAC: Ferric ammonium citrate

NMR: Nuclear Magnetic Resonance

Declarations

Ethics approval and consent to participate

All the experiments were obtained the approval of the Ethics Committee for Animal Experimentation of China Pharmaceutical University.

Consent for publication

Not applicable

Availability of data and materials

Not applicable

Competing interests

The authors declare that they have no competing interests.

Funding

This work was supported by the Project Program of Nature Science Foundation of Jiangsu Province of China (Grant No. BK20201329), the Fundamental Research Funds for the Central Universities (grant No.

2632018ZD01, No. 2632020ZD10), Innovation and Entrepreneurship Training Program for Undergraduate (No. 201910316220 and No. 202010316245), the Medical Science and Technology Research Project of Henan Province (no. SBGJ202003010), the Science and Technology Research Project of Henan Province (no. 202102310158) and the Priority Academic Program Development (PAPD) of Jiangsu Higher Education Institutions.

Authors' contributions

Lufeng Zheng, Feng Jiang and Tao Xi designed the research. Yuanyuan Lu and Feng Jiang approved the compounds. Yue Yang, Chunhua Zhang, Zhuolu Xia, Jing Liu, Xiangyu Cheng, Ting Wang, Qinqian Guo analyzed the data. Yue Yang, Chunhua Zhang performed the research. Yue Yang and Lufeng Zheng wrote the paper. All authors read and approved the final manuscript.

Acknowledgements

Not applicable

References

1. Chen W, Qin Y, Liu S: **Cytokines, breast cancer stem cells (BCSCs) and chemoresistance**. *Clinical and translational medicine* 2018, **7**(1):27.
2. Fiorentino S, Urueña C, Lasso P, Prieto K, Barreto A: **Phyto-Immunotherapy, a Complementary Therapeutic Option to Decrease Metastasis and Attack Breast Cancer Stem Cells**. *Front Oncol* 2020, **10**:1334.
3. Peitzsch C, Tyutyunnykova A, Pantel K, Dubrovska A: **Cancer stem cells: The root of tumor recurrence and metastases**. *Seminars in cancer biology* 2017, **44**:10-24.
4. Yang F, Xu J, Tang L, Guan X: **Breast cancer stem cell: the roles and therapeutic implications**. *Cellular and molecular life sciences : CMLS* 2017, **74**(6):951-966.
5. Yang Y, Li X, Wang T, Guo Q, Xi T, Zheng L: **Emerging agents that target signaling pathways in cancer stem cells**. *Journal of hematology & oncology* 2020, **13**(1):60.
6. Norsworthy KJ, By K, Subramaniam S, Zhuang L, Del Valle PL, Przepiorka D, Shen YL, Sheth CM, Liu C, Leong R *et al*: **FDA Approval Summary: Glasdegib for Newly Diagnosed Acute Myeloid Leukemia**. *Clinical cancer research : an official journal of the American Association for Cancer Research* 2019, **25**(20):6021-6025.
7. Beziat G, Ysebaert L: **Tagraxofusp for the Treatment of Blastic Plasmacytoid Dendritic Cell Neoplasm (BPDCN): A Brief Report on Emerging Data**. *OncoTargets and therapy* 2020, **13**:5199-5205.
8. Recalcati S, Gammella E, Cairo G: **Dysregulation of iron metabolism in cancer stem cells**. *Free radical biology & medicine* 2019, **133**:216-220.
9. Ozer U: **The role of Iron on breast cancer stem-like cells**. *Cellular and molecular biology (Noisy-le-Grand, France)* 2016, **62**(4):25-30.

10. Mai TT, Hamaï A, Hienzsch A, Cañeque T, Müller S, Wicinski J, Cabaud O, Leroy C, David A, Acevedo V *et al*: **Salinomycin kills cancer stem cells by sequestering iron in lysosomes**. *Nature chemistry* 2017, **9**(10):1025-1033.
11. Torti SV, Torti FM: **Iron and cancer: more ore to be mined**. *Nature reviews Cancer* 2013, **13**(5):342-355.
12. Bajbouj K, Shafarin J, Hamad M: **Estrogen-dependent disruption of intracellular iron metabolism augments the cytotoxic effects of doxorubicin in select breast and ovarian cancer cells**. *Cancer management and research* 2019, **11**:4655-4668.
13. Ma S, Henson ES, Chen Y, Gibson SB: **Ferroptosis is induced following siramesine and lapatinib treatment of breast cancer cells**. *Cell death & disease* 2016, **7**(7):e2307.
14. Chang VC, Cotterchio M, Khoo E: **Iron intake, body iron status, and risk of breast cancer: a systematic review and meta-analysis**. *BMC cancer* 2019, **19**(1):543.
15. Ma S, Dielschneider RF, Henson ES, Xiao W, Choquette TR, Blankstein AR, Chen Y, Gibson SB: **Ferroptosis and autophagy induced cell death occur independently after siramesine and lapatinib treatment in breast cancer cells**. *PLoS One* 2017, **12**(8):e0182921.
16. Corte-Rodríguez M, Blanco-González E, Bettmer J, Montes-Bayón M: **Quantitative Analysis of Transferrin Receptor 1 (TfR1) in Individual Breast Cancer Cells by Means of Labeled Antibodies and Elemental (ICP-MS) Detection**. *Analytical chemistry* 2019, **91**(24):15532-15538.
17. Miller LD, Coffman LG, Chou JW, Black MA, Bergh J, D'Agostino R, Jr., Torti SV, Torti FM: **An iron regulatory gene signature predicts outcome in breast cancer**. *Cancer Res* 2011, **71**(21):6728-6737.
18. Zhao B, Li X, Wang Y, Shang P: **Iron-dependent cell death as executioner of cancer stem cells**. *Journal of experimental & clinical cancer research : CR* 2018, **37**(1):79.
19. Versini A, Colombeau L, Hienzsch A, Gaillet C, Retailleau P, Debieu S, Müller S, Cañeque T, Rodriguez R: **Salinomycin Derivatives Kill Breast Cancer Stem Cells by Lysosomal Iron Targeting**. *Chemistry (Weinheim an der Bergstrasse, Germany)* 2020, **26**(33):7416-7424.
20. Versini A, Colombeau L, Hienzsch A, Gaillet C, Retailleau P, Debieu S, Muller S, Caneque T, Rodriguez R: **Salinomycin Derivatives Kill Breast Cancer Stem Cells via Lysosomal Iron Targeting**. *Chemistry (Weinheim an der Bergstrasse, Germany)* 2020.
21. Turcu AL, Versini A, Khene N, Gaillet C, Caneque T, Muller S, Rodriguez R: **DMT1 Inhibitors Kill Cancer Stem Cells by Blocking Lysosomal Iron Translocation**. *Chemistry (Weinheim an der Bergstrasse, Germany)* 2020.
22. Xu Y, Wang Q, Li X, Chen Y, Xu G: **Itraconazole attenuates the stemness of nasopharyngeal carcinoma cells via triggering ferroptosis**. *Environmental toxicology* 2021, **36**(2):257-266.
23. Sun J, Cheng X, Pan S, Wang L, Dou W, Liu J, Shi X: **Dichloroacetate attenuates the stemness of colorectal cancer cells via trigerring ferroptosis through sequestering iron in lysosomes**. *Environmental toxicology* 2020.
24. Guo Q, Wang T, Yang Y, Gao L, Zhao Q, Zhang W, Xi T, Zheng L: **Transcriptional Factor Yin Yang 1 Promotes the Stemness of Breast Cancer Cells by Suppressing miR-873-5p Transcriptional Activity**. *Molecular therapy Nucleic acids* 2020, **21**:527-541.

25. Lu, Yuanyuan, Wang, Linlin, Xiaobing, Xi, Tao, Liao, Jianmin, Zhixiang: **Design, combinatorial synthesis and biological evaluations of novel 3-amino-1'-((1-aryl-1H-1,2,3-triazol-5-yl)methyl)-2'-oxospiro[benzo[a] pyrano[2,3-c]phenazine-1,3'-indoline]-2-carbonitrile antitumor hybrid molecules**. *European journal of medicinal chemistry* 2017.
26. Ghafouri-Fard S, Taheri M: **UCA1 long non-coding RNA: An update on its roles in malignant behavior of cancers**. *Biomedicine & pharmacotherapy = Biomedecine & pharmacotherapie* 2019, **120**:109459.
27. Klinge CM: **Non-Coding RNAs in Breast Cancer: Intracellular and Intercellular Communication**. *Non-coding RNA* 2018, **4**(4).
28. Gao M, Yi J, Zhu J, Minikes AM, Monian P, Thompson CB, Jiang X: **Role of Mitochondria in Ferroptosis**. *Molecular cell* 2019, **73**(2):354-363.e353.
29. Eun K, Ham SW, Kim H: **Cancer stem cell heterogeneity: origin and new perspectives on CSC targeting**. *BMB reports* 2017, **50**(3):117-125.
30. Wang T, Shigdar S, Gantier MP, Hou Y, Wang L, Li Y, Shamaileh HA, Yin W, Zhou SF, Zhao X *et al*: **Cancer stem cell targeted therapy: progress amid controversies**. *Oncotarget* 2015, **6**(42):44191-44206.
31. O'Conor CJ, Chen T, González I, Cao D, Peng Y: **Cancer stem cells in triple-negative breast cancer: a potential target and prognostic marker**. *Biomarkers in medicine* 2018, **12**(7):813-820.
32. Kim SE, Zhang L, Ma K, Riegman M, Chen F, Ingold I, Conrad M, Turker MZ, Gao M, Jiang X *et al*: **Ultrasmall nanoparticles induce ferroptosis in nutrient-deprived cancer cells and suppress tumour growth**. *Nature nanotechnology* 2016, **11**(11):977-985.
33. Kurz T, Terman A, Gustafsson B, Brunk UT: **Lysosomes in iron metabolism, ageing and apoptosis**. *Histochemistry and cell biology* 2008, **129**(4):389-406.
34. Su S, Chen J, Yao H, Liu J, Yu S, Lao L, Wang M, Luo M, Xing Y, Chen F *et al*: **CD10(+)GPR77(+) Cancer-Associated Fibroblasts Promote Cancer Formation and Chemoresistance by Sustaining Cancer Stemness**. *Cell* 2018, **172**(4):841-856.e816.
35. Rycaj K, Tang DG: **Cell-of-Origin of Cancer versus Cancer Stem Cells: Assays and Interpretations**. *Cancer Res* 2015, **75**(19):4003-4011.
36. Schonberg DL, Miller TE, Wu Q, Flavahan WA, Das NK, Hale JS, Hubert CG, Mack SC, Jarrar AM, Karl RT *et al*: **Preferential Iron Trafficking Characterizes Glioblastoma Stem-like Cells**. *Cancer cell* 2015, **28**(4):441-455.
37. Pietrangelo A: **Iron and the liver**. *Liver international : official journal of the International Association for the Study of the Liver* 2016, **36 Suppl 1**:116-123.
38. Kremastinos DT, Farmakis D: **Iron overload cardiomyopathy in clinical practice**. *Circulation* 2011, **124**(20):2253-2263.
39. Raghupathy R, Manwani D, Little JA: **Iron Overload in Sickle Cell Disease**. *Advances in Hematology* 2010, **2010**:272940.

Figures

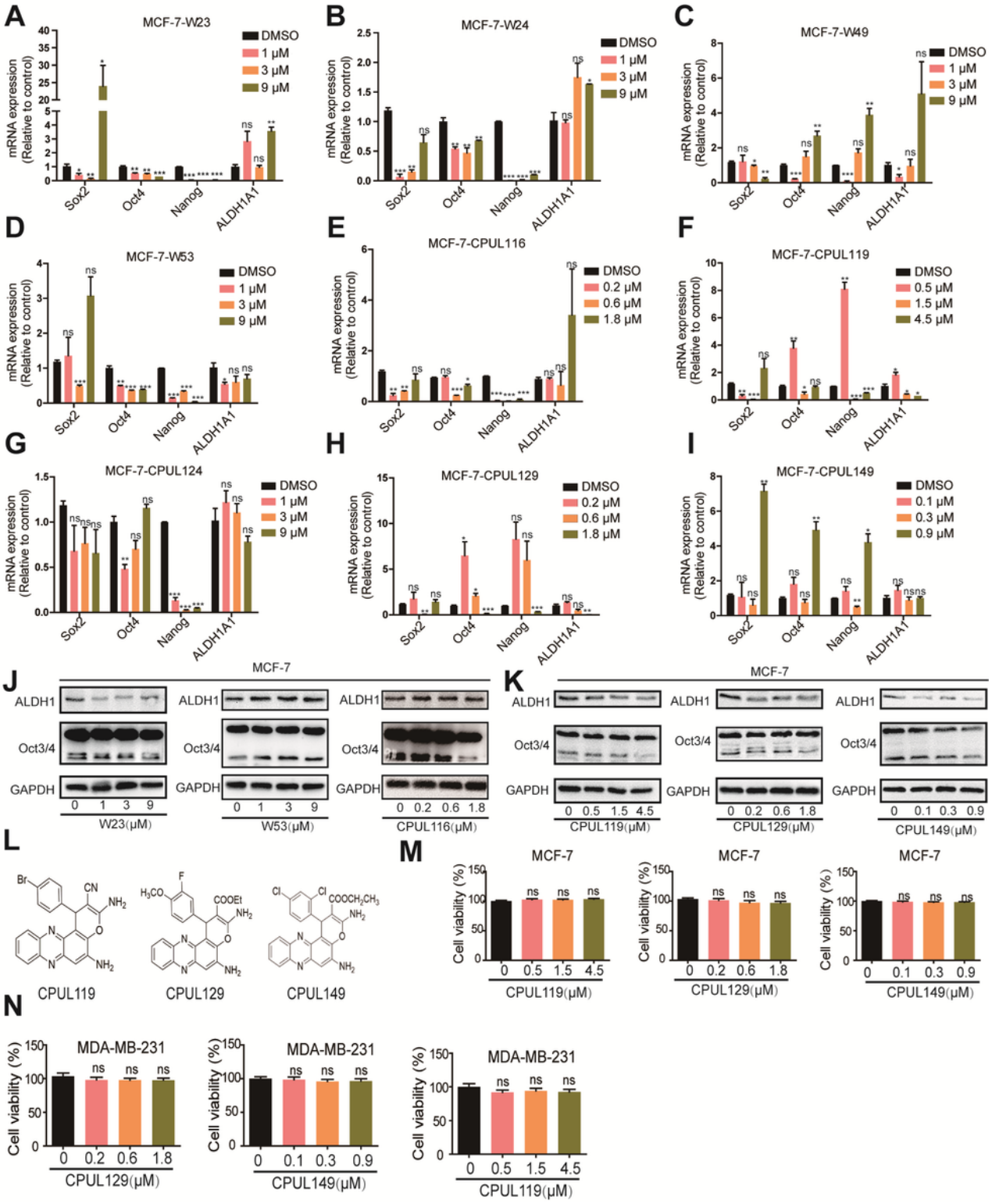

Figure 1

Identification of CPUL119, CPUL129 and CPUL149 as a novel small molecular targeting BCSCs. (A-I) qPCR analysis on the expression of stemness markers (Sox2, Oct4, Nanog, and ALDH1A1) of MCF-7 cells treated with or without compounds for 48 h. (J-K) Western blot analysis the protein expression of

stemness markers in the cell described in (A). (L) The structure of CPUL119, CPUL129 and CPUL149. (M, N) Cell viability was detected in cells treated with or without CPUL119, CPUL129 and CPUL149 for 48 h by MTT. Data are presented as the mean ± SD, n = 3, *p < 0.05, **p < 0.01, ***p < 0.001 vs. control group.

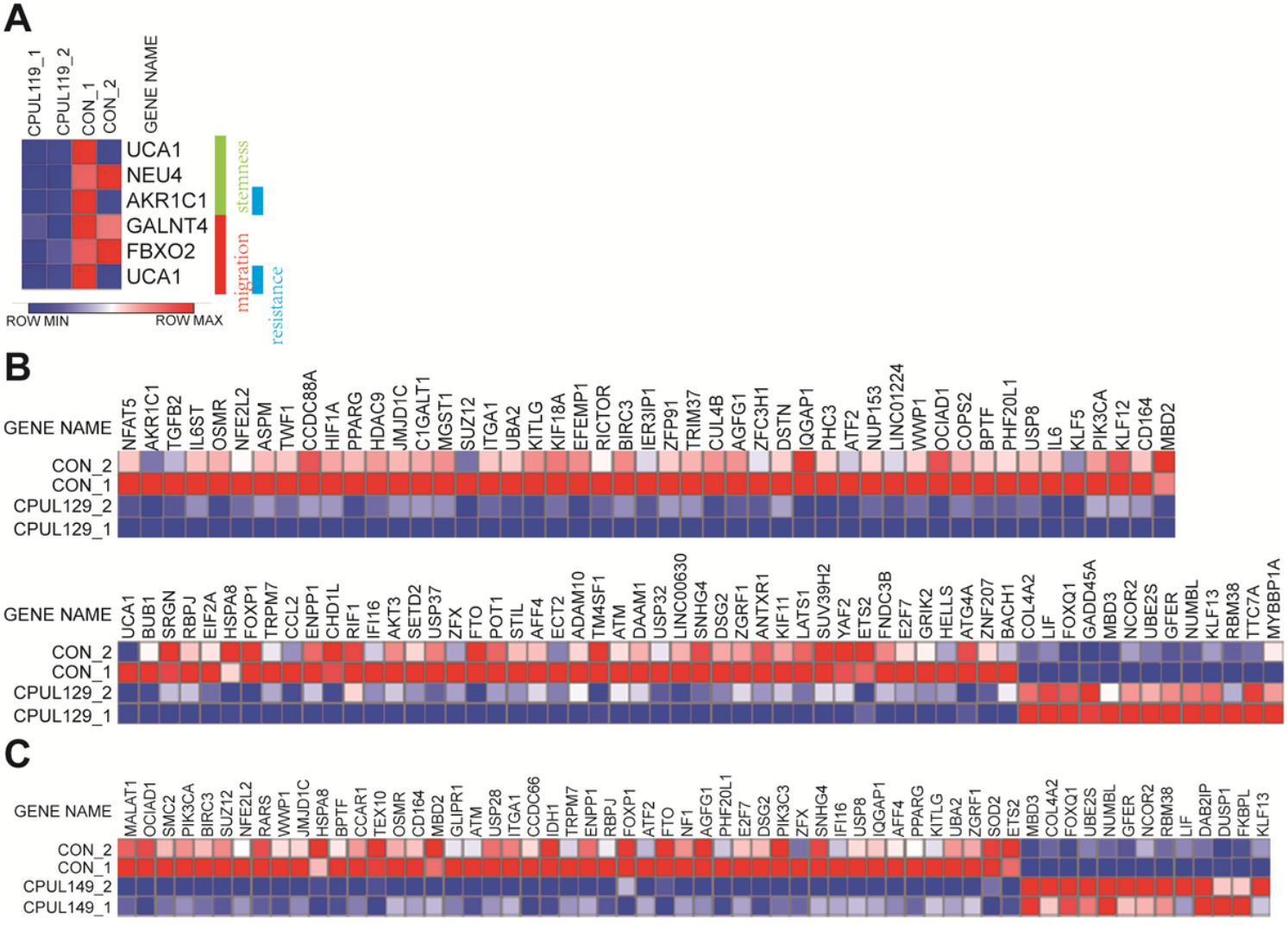

Figure 2

The transcriptome analysis after MD-MB-231 cells treated with or without CPUL 119, CPU L129 and CPUL 149. (A) Expression of stemness-, migration- and chemoresistance- related gene was analyzed in cells treated with or without CPUL119 treatment based on RNA-seq analysis. (B and C) Expression of stemness-related genes was changed in cells treated with or without CPUL129 (B) and CPUL149 (C) based on RNA-seq analysis.

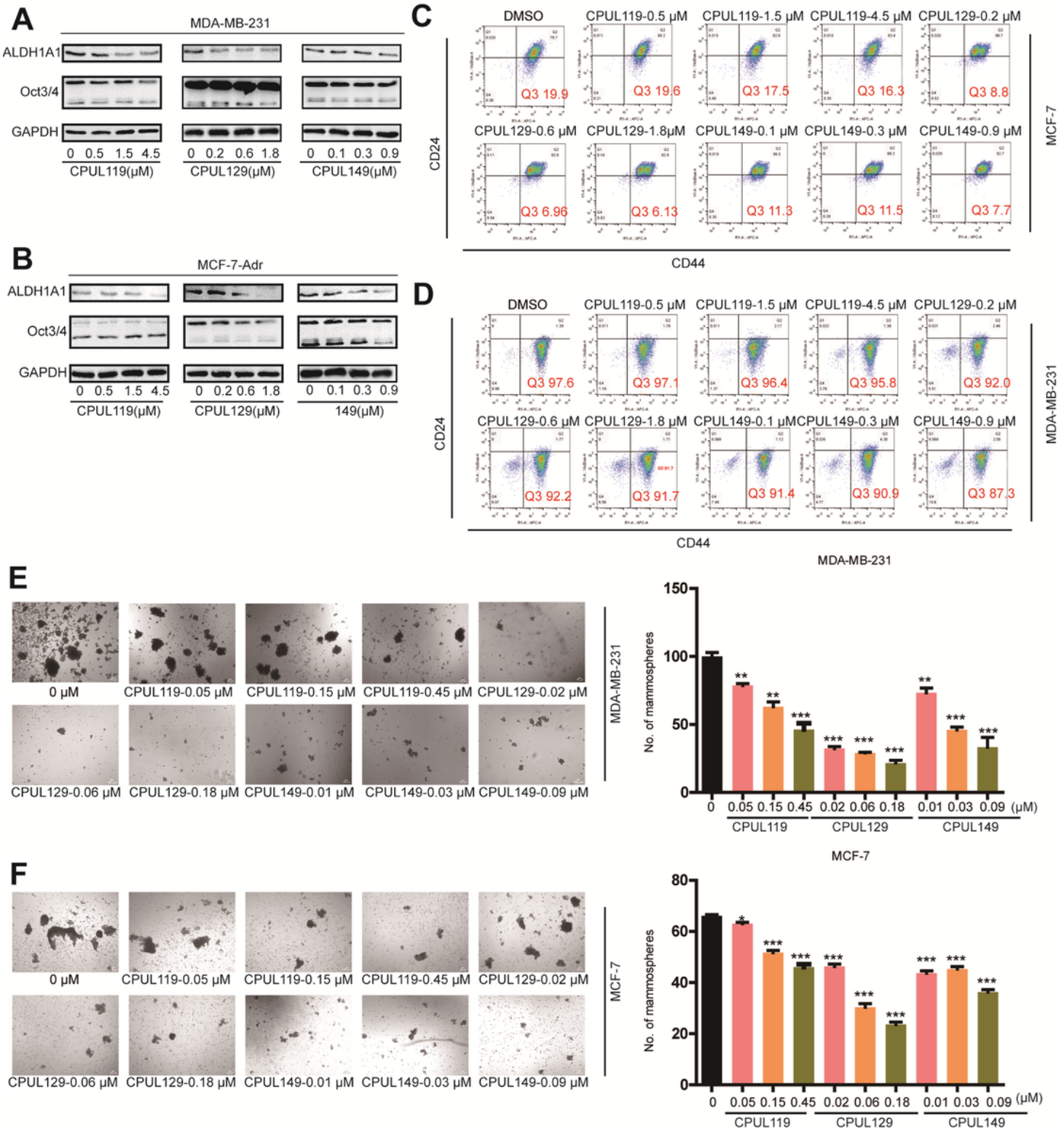

Figure 3

CPUL119, CPUL129 and CPUL149 inhibit the stemness of breast cancer stem cells. (A and B) The protein expression of stemness markers was detected in MDA-MB-231 cells and MCF-7-Adr cells after being treated with CPUL119, CPUL129 and CPUL149 by Western blot analysis. (C and D) The subpopulation of CD44+/CD24- was analyzed by flow cytometry in cells described in (A). (E and F) The spheroid formation ability (size and number) was evaluated in MCF-7 and MDA-MB-231 cells treated with or without

CPUL119, CPUL129 and CPUL149, respectively. At the same time, the correlated quantification of mammosphere formation was list at the right. Data are presented as the mean ± SD, n = 3, *p < 0.05, **p < 0.01, ***p < 0.001 vs. control group.

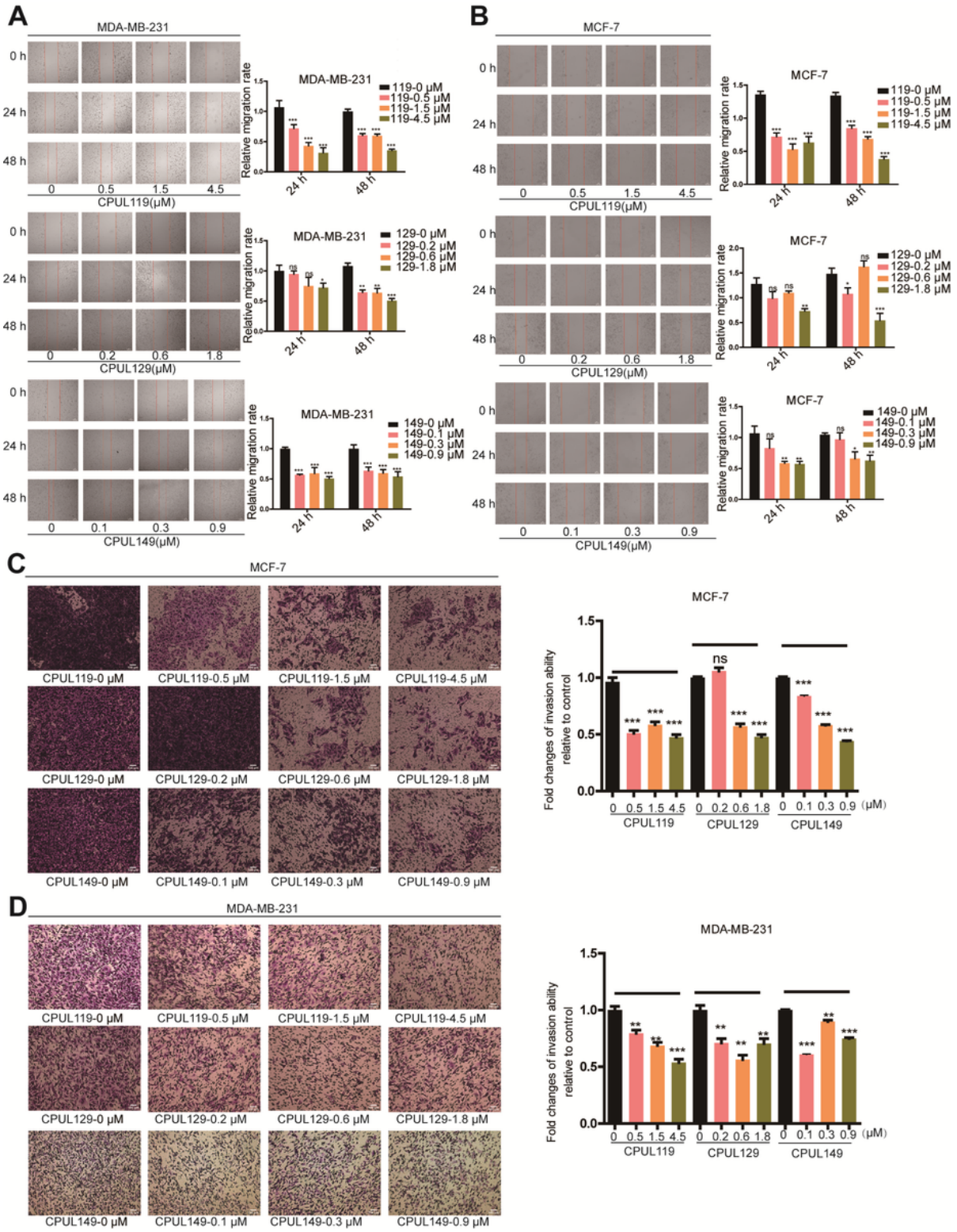

Figure 4

CPUL119, CPUL129 and CPUL149 inhibit the migration and invasion of breast cancer cells. (A and B) The migration ability was measured and quantified by wound-healing analysis in cells treated with or without

CPUL119, CPUL129 and CPUL149 for 24 h and 48 h, respectively. (C and D) The invasion ability was analyzed and quantified by transwell-invasion analysis in the cells described in (A). Data are presented as the mean ± SD, n = 3, *p < 0.05, **p < 0.01, ***p < 0.001 vs. control group.

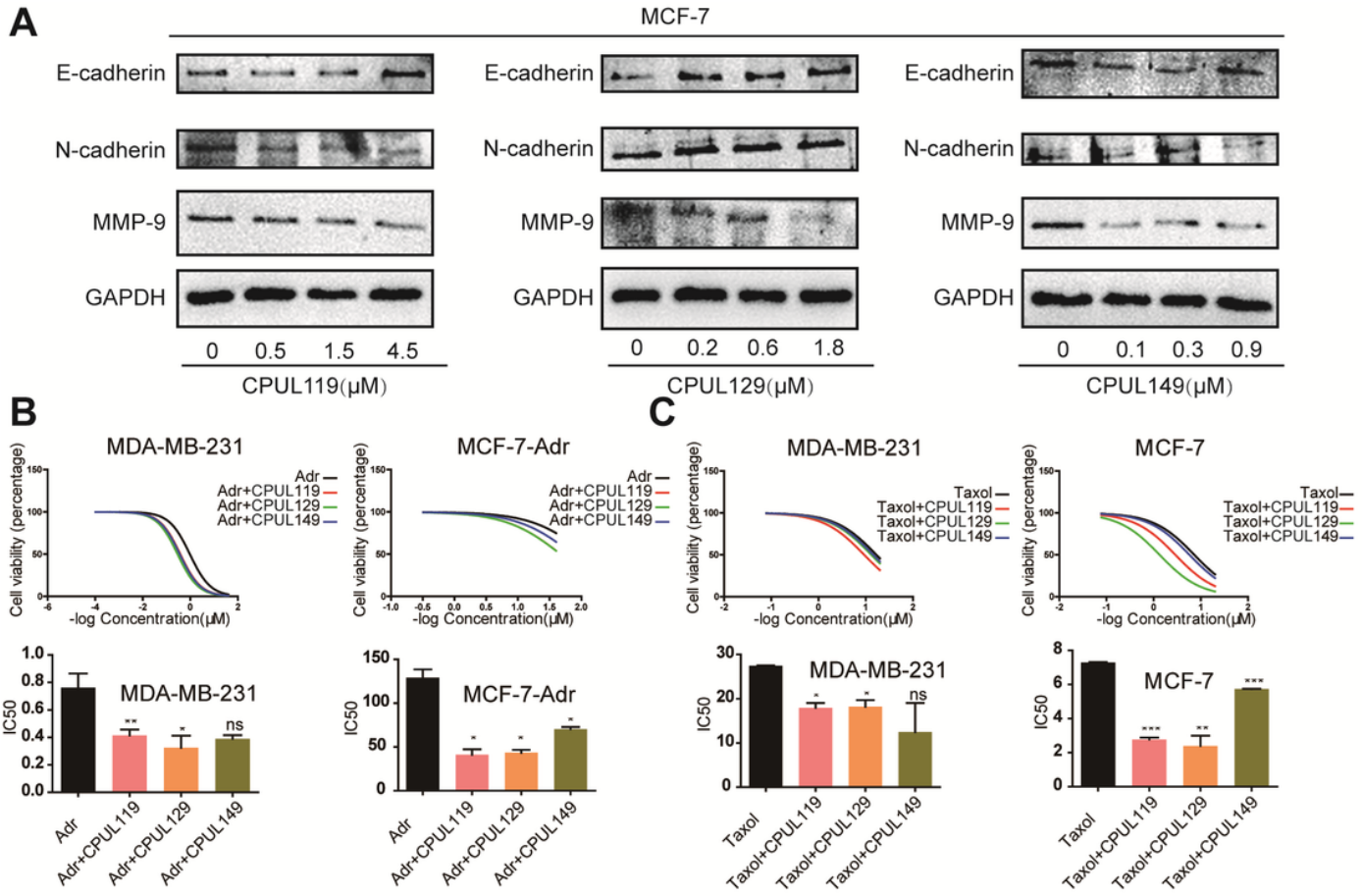

Figure 5

CPUL119, CPUL129 and CPUL149 inhibit the EMT process and drug resistance of breast cancer cells. (A) The protein expression of EMT markers (E-cadherin, N-cadherin and MMP9) were measured in MCF-7 cells treated with or without CPUL119, CPUL129 and CPUL149 for 48 h. (B and C) Cell viability was determined in cells treated with CPUL119 (4.5 μM), CPUL129 (1.8 μM) and CPUL149 (0.9 μM) combined with Adr or Taxol through MTT analysis. Data are presented as the mean ± SD, n = 3, *p < 0.05, **p < 0.01, ***p < 0.001 vs. control group.

A

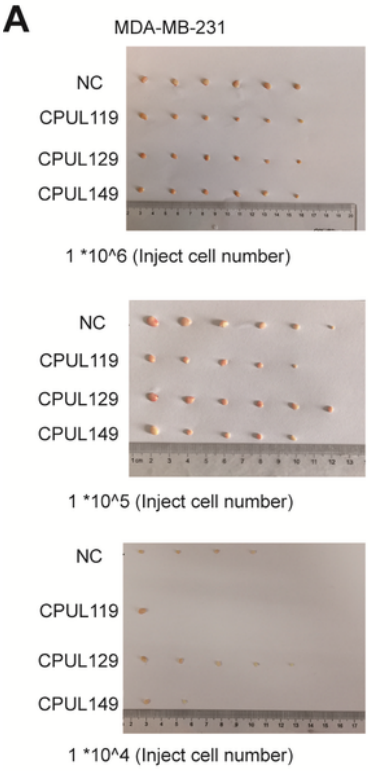

B

Inject cell number	NC	CPUL119	CPUL129	CPUL149
1 *10^4	4/6	1/6	5/6	2/6
1 *10^5	6/6	5/6	6/6	5/6
1 *10^6	6/6	6/6	6/6	6/6

Confidence intervals for 1/(stem cell frequency)

Group	Lower	Estimate	Upper
CPUL119	135606	55613	22808
CPUL129	15150	5582	2057
CPUL149	109684	44788	18288
NC	25444	9100	3255

C

Group 1	Group 2	Chisq	DF	Pr (> Chisq)
CPUL119	NC	6.29	1	0.0122
CPUL129	NC	0.451	1	0.502
CPUL149	NC	5.01	1	0.0252

D

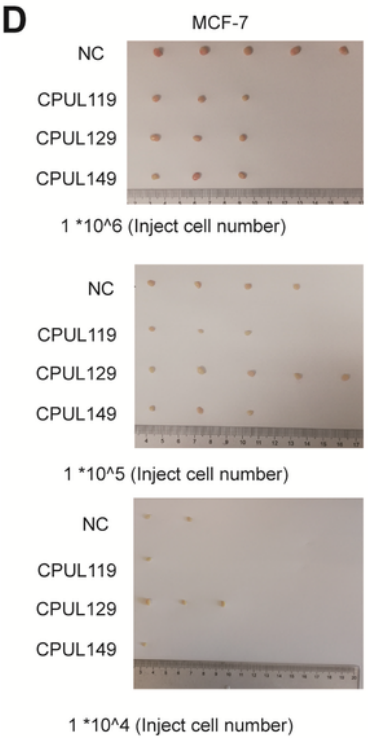

E

Inject cell number	NC	CPUL119	CPUL129	CPUL149
1 *10^4	2/6	1/6	3/6	1/6
1 *10^5	4/6	3/6	5/6	3/6
1 *10^6	5/6	3/6	3/6	3/6

Confidence intervals for 1/(stem cell frequency)

Group	Lower	Estimate	Upper
CPUL119	1619501	662497	271011
CPUL129	957919	391439	159956
CPUL149	1619501	662497	271011
NC	623671	228602	83793

F

Group 1	Group 2	Chisq	DF	Pr (> Chisq)
CPUL119	NC	3.94	1	0.0471
CPUL129	NC	1.19	1	0.276
CPUL149	NC	3.94	1	0.0471

Figure 6

CPUL119, CPUL129 and CPUL149 inhibit the stemness of breast cancer stem cells in vivo. (A and B) Images of tumors harvested when serially diluted MDA-MB-231 cells with or without CPUL119, CPUL129 or CPUL149 pre-treatment, respectively (A) and tumor formation rate was evaluated (B). (C) TIC (Tumor Initiation Cells) frequencies (left), χ2 values, and associated probabilities (right) of cells described in (A). (D and E) Images of tumors harvested when serially diluted MCF-7 cells with or without CPUL119,

CPUL129 or CPUL149 pre-treatment, respectively (D) and tumor formation rate was evaluated (E). (F) TIC (Tumor Initiation Cells) frequencies (left), χ2 values, and associated probabilities (right) of cells described in (D)

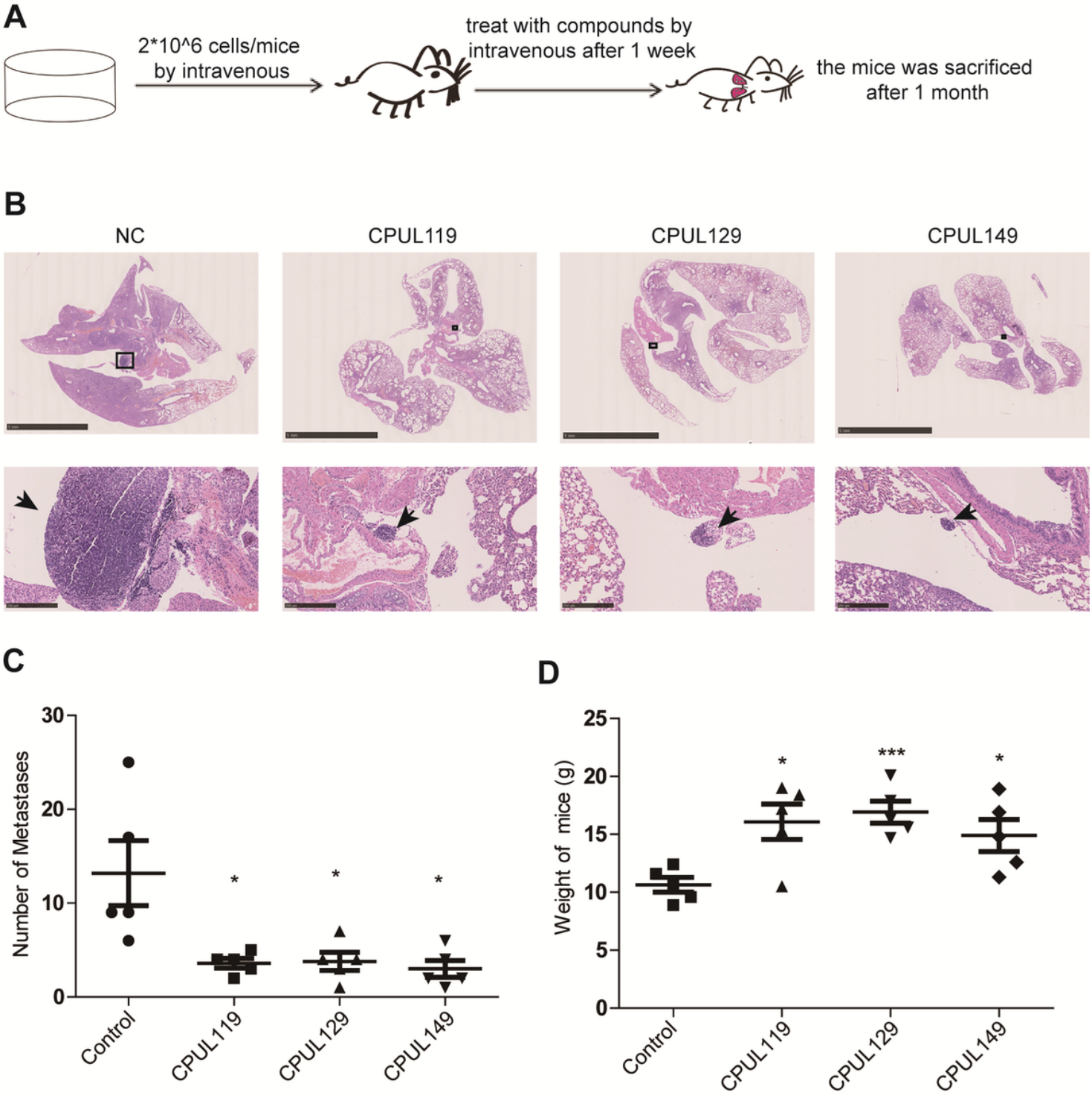

Figure 7

CPUL119, CPUL129 and CPUL149 inhibit the metastasis of breast cancer cells in vivo. (A) The diagram to construct the lung metastatic model in nude mice. (B) H&E staining to lungs derived from mice treated with or without CPUL119, CPUL129 or CPUL149, respectively. (C) The numbers of metastatic nodules

were quantified. (D) The weight of nude mice was measured when sacrificed. Data are presented as the mean ± SD, n = 5, *p < 0.05, ***p < 0.001 v vs. control group.

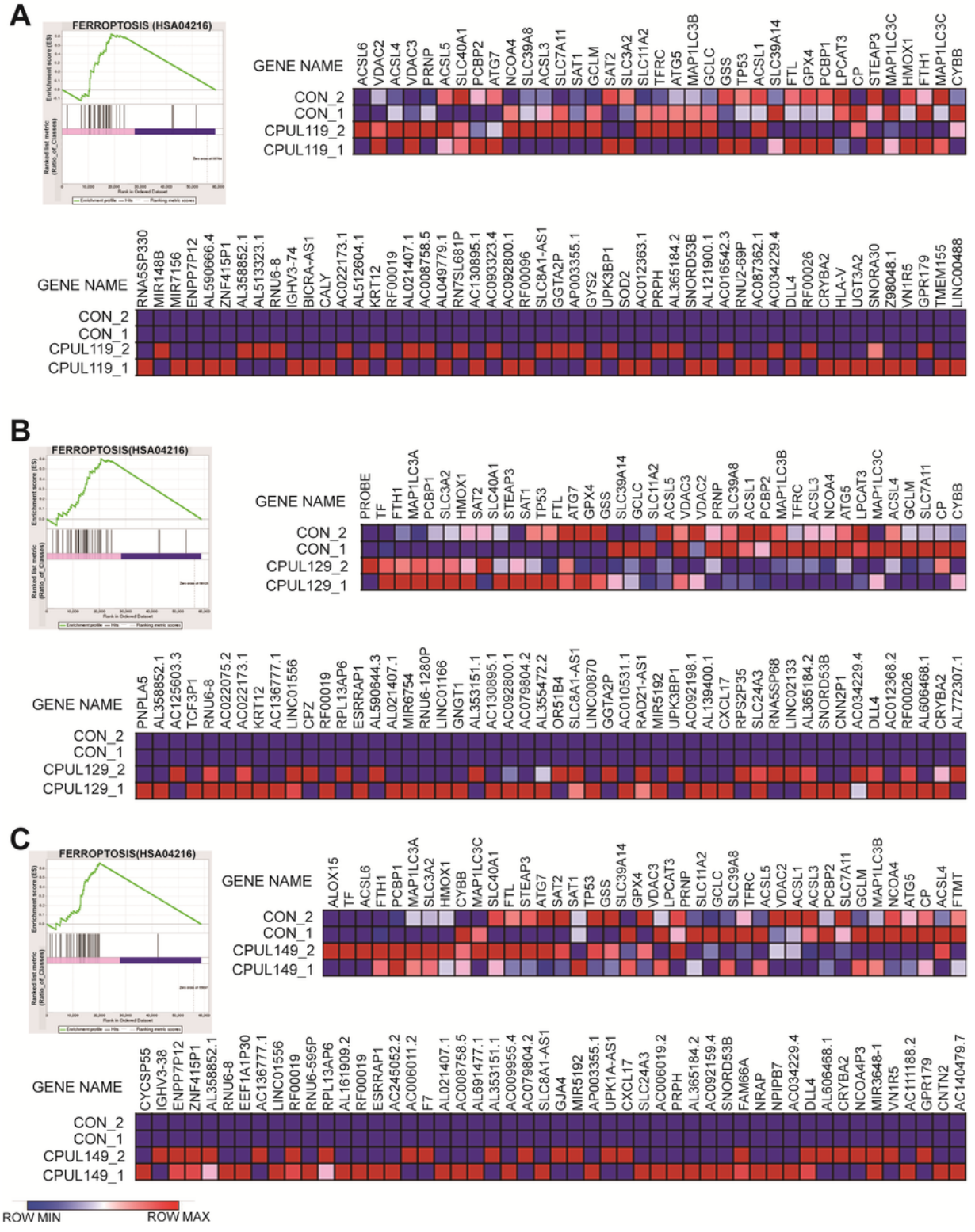

Figure 8

The transcriptome analysis after MD-MB-231 cells treated with or without CPUL119, CPUL129 and CPUL149. (A-C) GSEA enrichment analysis showed that the genes involved in the ferroptosis pathways

were enriched in MDA-MB-231 cells treated with CPUL119, CPUL129 or CPUL149, respectively. And the expression of ferroptosis-related genes was changed based on RNA-seq analysis.

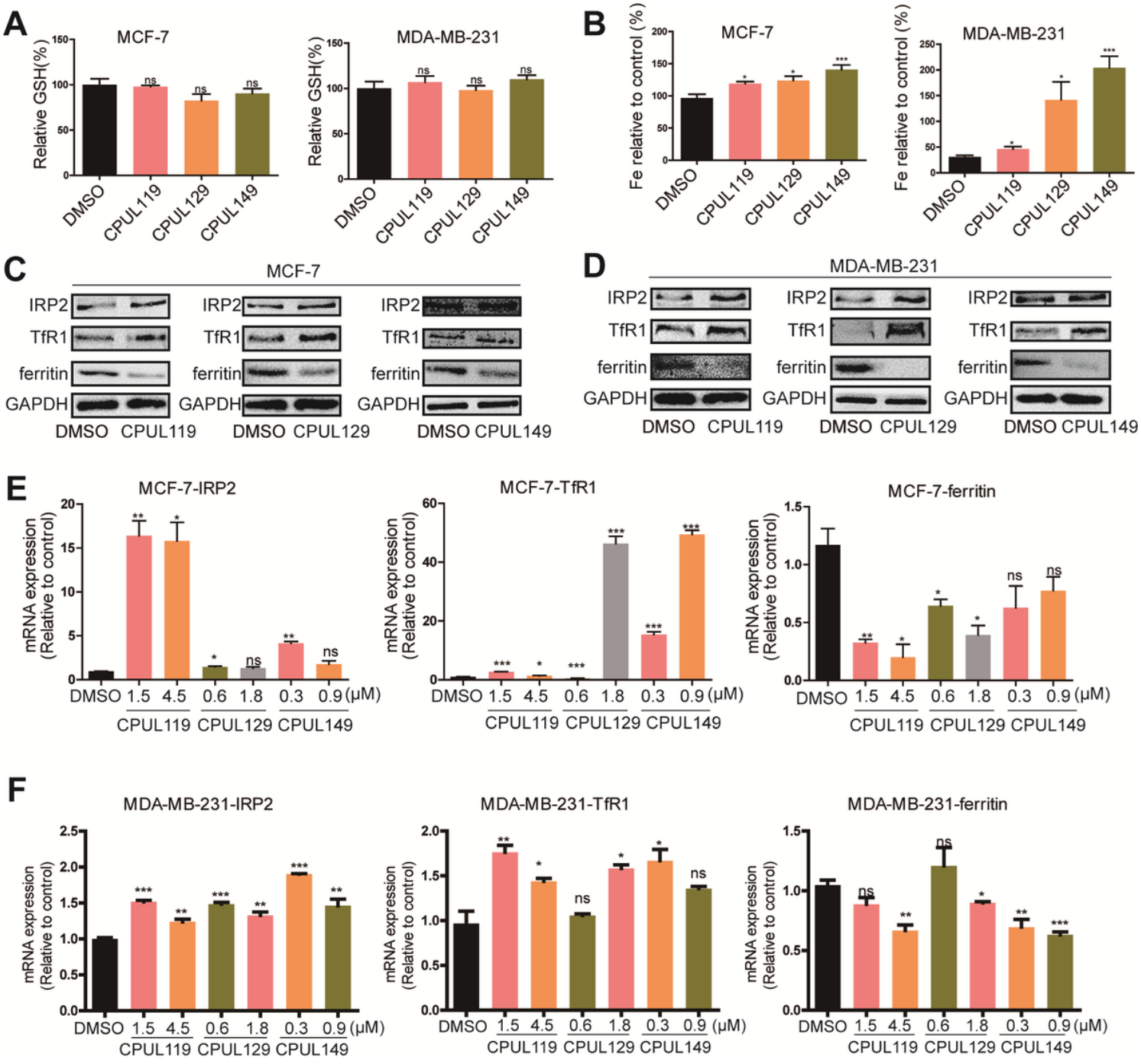

Figure 9

CPUL119, CPUL129 and CPUL149 regulates the iron hemostasis and ferroptosis in breast cancer cells. (A) The GSH level was detected in MCF-7 and MDA-MB-231 cells treated with or without CPUL119, CPUL129 and CPUL149 for 48 h. (B) The concentration of iron was measured in MCF-7 and MDA-MB-231 cells treated with or without CPUL119, CPUL129 and CPUL149 for 48 h. (C-F) The protein expression of iron metabolism-related genes including IRP2, TfR1 and ferritin was analyzed by western blot and qPCR

in MCF-7 and MDA-MB-231 cells treated with or without CPUL119, CPUL129 and CPUL149 for 48 h. Data are presented as the mean ± SD, n = 3, *p < 0.05, **p < 0.01, ***p < 0.001 vs. DMSO group.

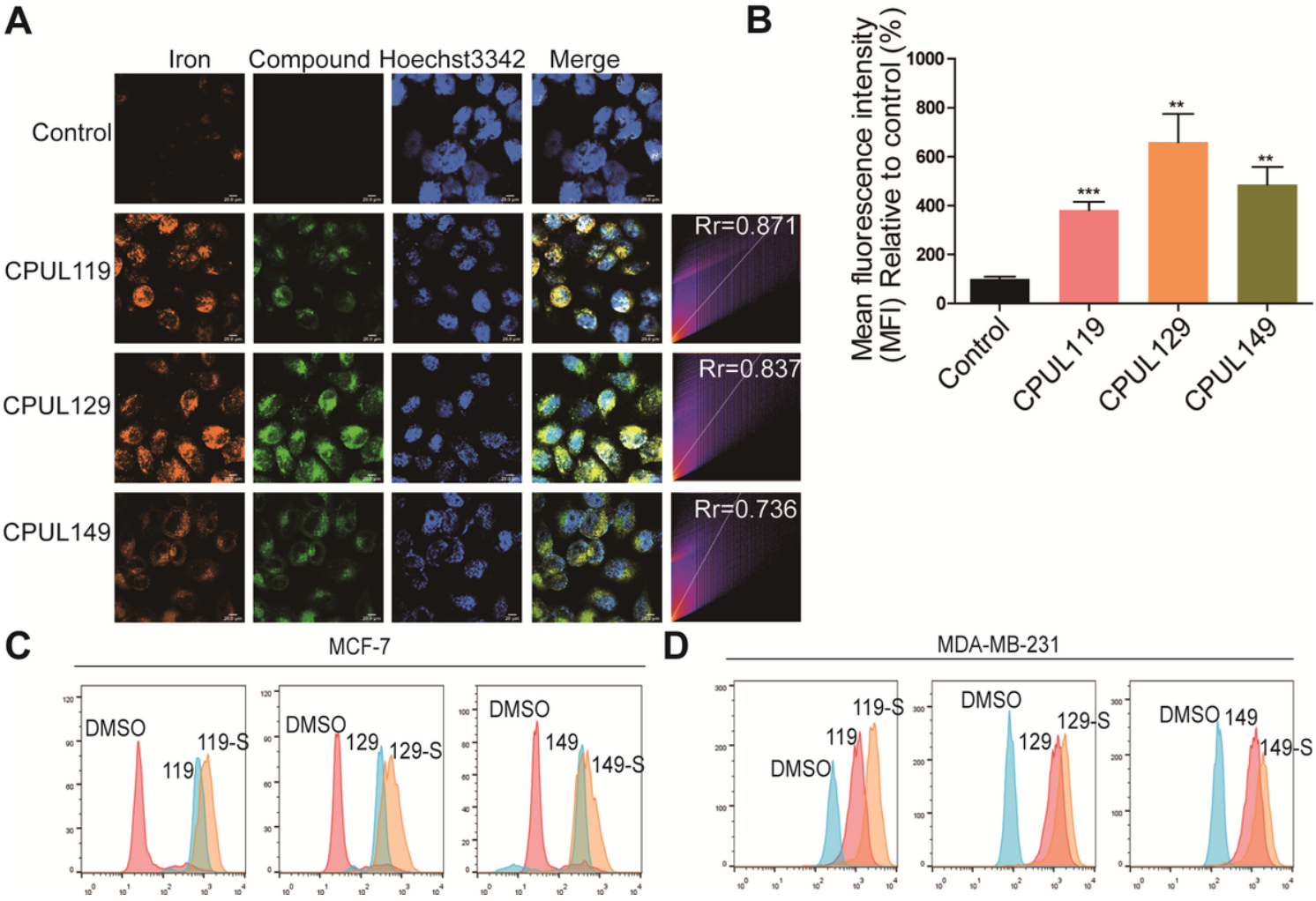

Figure 10

CPUL119, CPUL129 and CPUL149 regulates the iron hemostasis and ferroptosis in breast cancer cells. (A) The localization of iron and CPUL119, CPUL129 and CPUL149 was detected using a Laser confocal microscope and the colocalization coefficient was analyzed. (B) Quantification of iron concentration in A. (C-D) The ROS level was measured in MCF-7 and MDA-MB-231 cells treated with or without CPUL119, CPUL129 and CPUL149 for 48 h. Compound-S represents the cell stained with ROS probe. Data are presented as the mean ± SD, n = 3, **p < 0.01, ***p < 0.001 vs. control group.

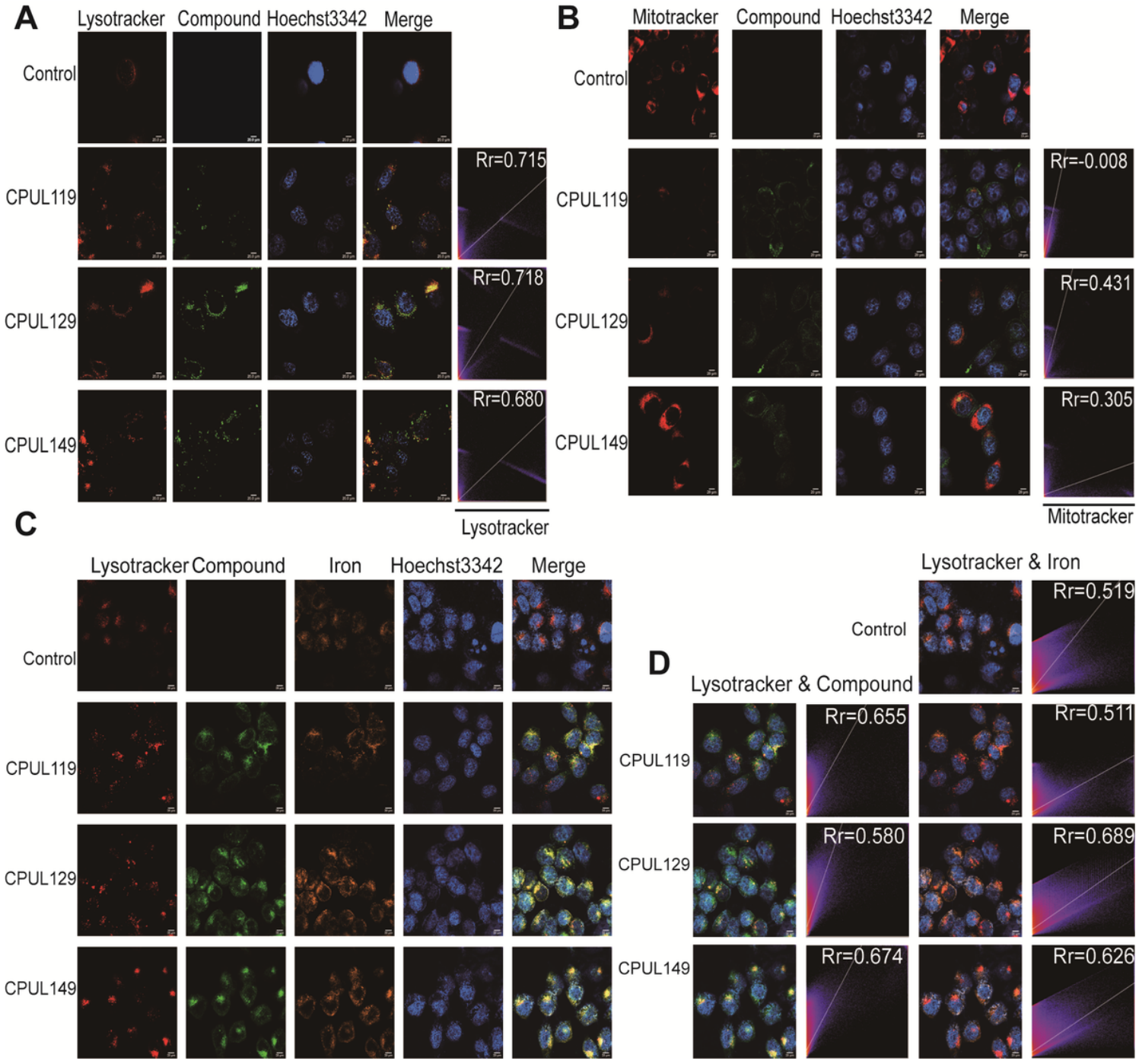

Figure 11

CPUL119, CPUL129 and CPUL149 interact and sequester iron in lysosomes in breast cancer cells. (A and B) The localization of CPUL119, CPUL129 and CPUL149 was determined using lysosome probe (Lysotracker) and mitochondrion (Mitotracker) probe, and the colocalization coefficient was analyzed. (C) The co-localization of CPUL119, CPUL129 or CPUL149 and iron was evaluated. (D) The co-localization was quantified with Image J. Data are presented as the mean ± SD, n = 3, *p < 0.05, **p < 0.01, ***p < 0.001 vs. control group.

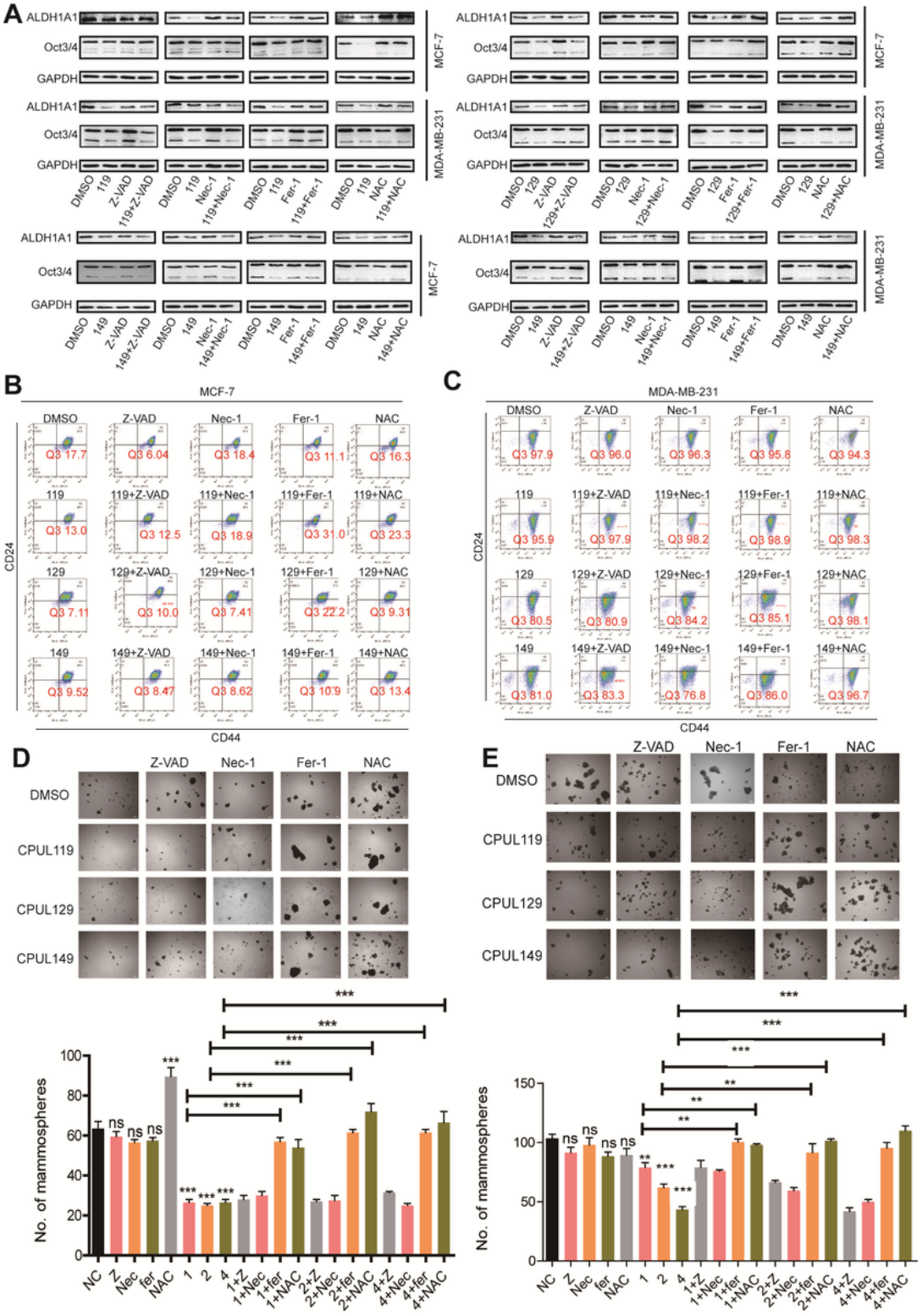

Figure 12

CPUL119, CPUL129 and CPUL149 attenuates the stemness of breast cancer cells partially through triggering ferroptosis. (A) The expression of stemness markers was detected in MCF-7 and MDA-MB-231 cells treated as indicated. (B and C) The subpopulation of CD44+/CD24- were analyzed in MCF-7 cells and MDA-MB-231 cells as depicted in (A) by flow cytometry. (D and E) The spheroid formation capacity

was evaluated and quantified in MCF-7 and MDA-MB-231 cells as depicted in (A). Data are presented as the mean ± SD, n = 3, *p < 0.05, **p < 0.01, ***p < 0.001 vs. DMSO group.

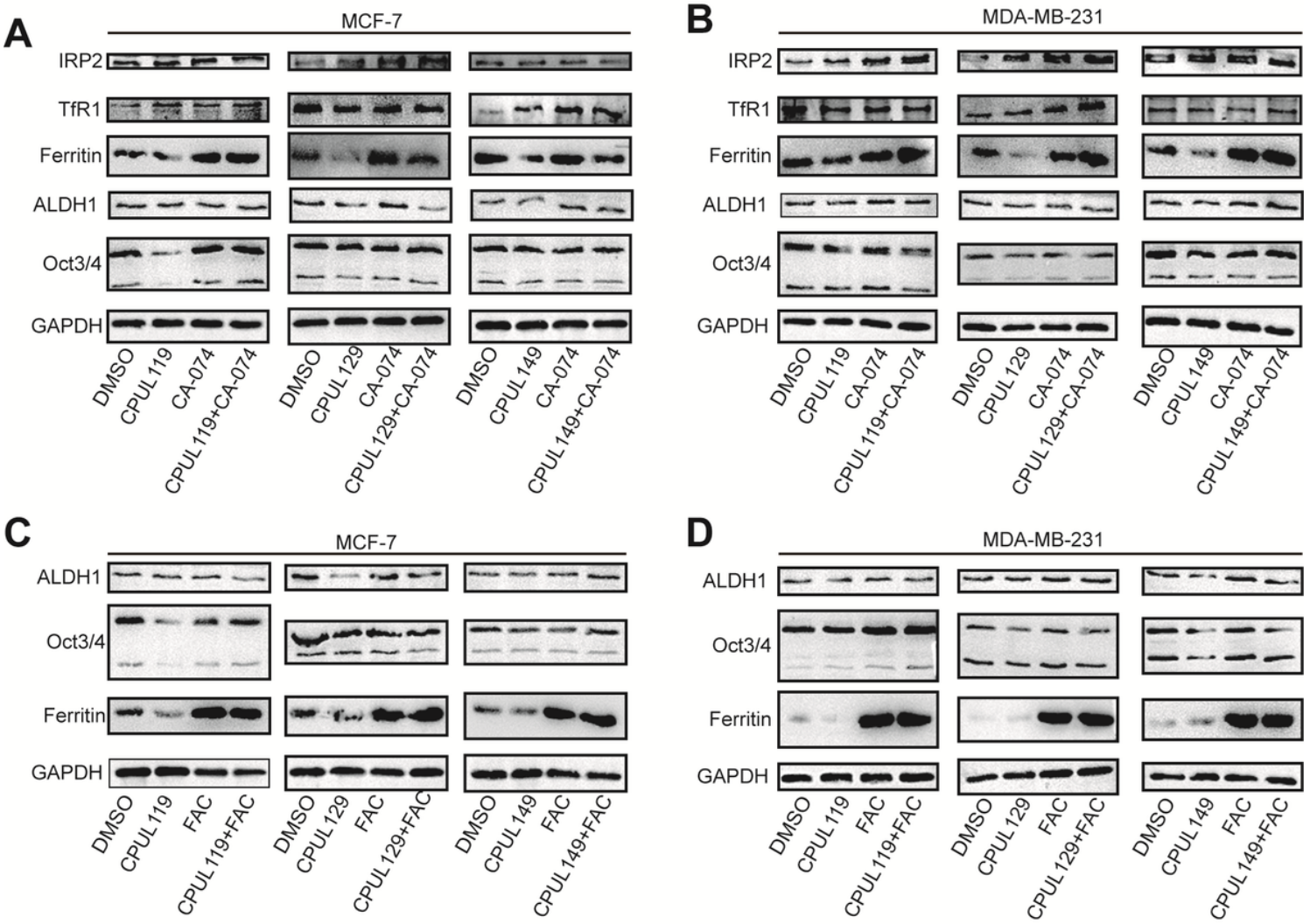

Figure 13

CPUL119, CPUL129 and CPUL149 attenuates the stemness of breast cancer cells partially through triggering ferroptosis. (A and B) Western blot analysis on the iron regulatory genes and stemness markers in MCF-7 and MDA-MB-231 cells treated with CPUL119, CPUL129, CPUL149 as well as CA-074 or not. (C and D) Western blot analysis on the ferritin and stemness marker expression in MCF-7 and MDA-MB-231 cells treated with CPUL119, CPUL129, CPUL149 as well as FAC (60 μM) or not. Data are presented as the mean ± SD, n = 3, *p < 0.05, **p < 0.01, ***p < 0.001 vs. DMSO/119/129/149 group.

Supplementary Files

This is a list of supplementary files associated with this preprint. Click to download.

- Supplementarymaterial.doc